Available online at www.sciencedirect.com
ScienceDirect
Journal of Organometallic Chemistry 692 (2007) 217–224
Journal of Organometallic Chemistry
www.elsevier.com/locate/jorganchem

Effects of bulky substituent groups on the Si–Si triple bonding in RSi≡SiR and the short Ga–Ga distance in Na_2[RGaGaR]: A theoretical study

Nozomi Takagi, Shigeru Nagase *

Department of Theoretical Molecular Science, Institute for Molecular Science, Myodaiji, Okazaki 444-8585, Japan

Received 6 June 2006; received in revised form 27 July 2006; accepted 1 August 2006
Available online 9 September 2006

Abstract

The steric and electronic effects of bulky aryl and silyl groups on the Si–Si triple bonding in RSi≡SiR and the short Ga–Ga distance in Na_2[RGaGaR] are investigated by density functional calculations. As typical bulky groups, Tbt = C_6H_2-2,4,6-{$CH(SiMe_3)_2$}$_3$, Ar′ = C_6H_3-2,6-(C_6H_3-2,6-*i*Pr_2)$_2$, Ar* = C_6H_3-2,6-(C_6H_2-2,4,6-*i*Pr_3)$_2$, SiMe(Si*t*Bu_3)$_2$, and Si*i*PrDis$_2$ (Dis = $CH(SiMe_3)_2$) are investigated and characterized. The importance of large basis sets is emphasized for density functional calculations.

Keywords: Substituent effect; Bulky group; Si–Si triple bond; Ga–Ga distance; Density functional calculation

1. Introduction

Multiple bonds between heavier main group elements have long attracted widespread interest, as summarized in reviews [1]. Among these, triple bonds between heavier group 14 elements have been the focus of interest as challenging synthetic targets [1]. The major difficulty in the synthesis and isolation of the heavier analogues of alkyne (RE≡ER: E = Si, Ge, Sn, and Pb) as stable compounds is ascribed to the high reactivities toward isomerization and dimerization. To suppress these reactivities, substituent effects have been extensively investigated by theoretical calculations [2]. Bulky aryl groups such as Tbt = C_6H_2-2,4,6-{$CH(SiMe_3)_2$}$_3$ and Ar* = C_6H_3-2,6-(C_6H_2-2,4,6-*i*Pr_3)$_2$ have been suggested as sterically promising substituents [2]. By using these bulky aryl groups as well as the slightly different groups, the Ge [3,4], Sn [5], and Pb [6] analogues of alkyne have been successfully synthesized and isolated.

Theoretical calculations have shown that electropositive silyl groups are electronically more effective in synthesizing a less trans-bent RE≡ER structure with a short E–E bond [2]. Therefore, the availability of silyl groups, which are bulky enough to prevent isomerization and dimerization, has been anticipated. By developing the so-called megasilyl group, SiMe(Si*t*Bu_3)$_2$, the probable synthesis of (Si*t*Bu_3)$_2$-MeSiSi≡SiSiMe(Si*t*Bu_3)$_2$ has been suggested from ^{29}Si NMR, mass spectrometry, and trapping experiment [7,2f,8], though its isolation has been unsuccessful. In contrast, Sekiguchi and co-workers have recently achieved the first isolation and characterization for Dis$_2$*i*PrSiSi≡Si-Si*i*PrDis$_2$ (Dis = $CH(SiMe_3)_2$) [9]. On the other hand, the synthesis and isolation of RSi≡SiR have not been reported for R = bulky aryl groups.

In 1997, Robinson and co-workers reported the synthesis and isolation of a novel compound, Na_2[Ar*GaGaAr*], as the first example of a triple bond between heavier group 13 elements [10]. Although the Ga–Ga distance of 2.319 Å is the shortest on record, the simple assignment of a Ga–Ga triple bond has been repeatedly debated [11]. We have disclosed that several factors play an important role in the short Ga–Ga distance and the heart of the compound is

* Corresponding author.
E-mail address: nagase@ims.ac.jp (S. Nagase).

0022-328X/$ - see front matter © 2006 Elsevier B.V. All rights reserved.
doi:10.1016/j.jorganchem.2006.08.089

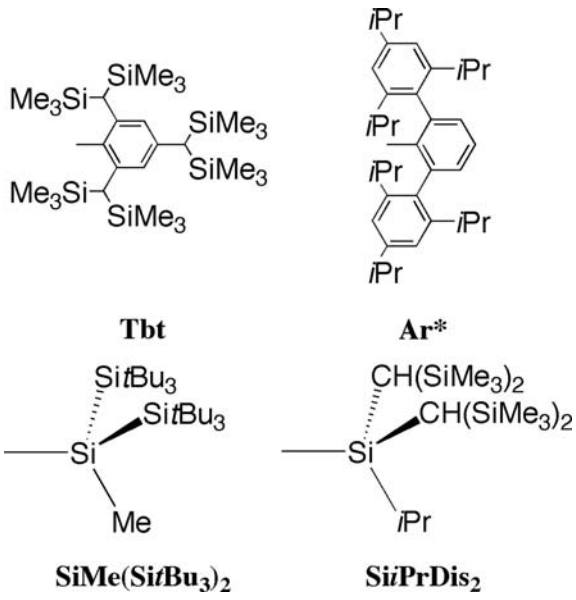

Chart 1.

a Ga_2Na_2 cluster rather than a simple Ga–Ga bond [12]. A number of theoretical calculations have been performed for the simple model systems where the bulky Ar* group is replaced by small groups such as H, CH_3, and Ph, because of the size of Na_2[Ar*GaGaAr*] [11]. However, the short Ga–Ga distance of 2.319 Å has never been well reproduced by model calculations.

In this study, we have investigated systematically the steric and electronic effects of bulky aryl and silyl substituent groups on the Si–Si triple bonding in RSi≡SiR (disilyne) and the short Ga–Ga distance in Na_2[RGaGaR] using density functional calculations with large basis sets. For this purpose, Tbt = C_6H_2-2,4,6-{$CH(SiMe_3)_2$}$_3$, Ar′ = C_6H_3-2,6-(C_6H_3-2,6-*i*Pr_2)$_2$, Ar* = C_6H_3-2,6-(C_6H_2-2,4,6-*i*Pr_3)$_2$, SiMe(Si*t*Bu_3)$_2$, and Si*i*PrDis$_2$ (Dis = $CH(SiMe_3)_2$) are investigated as typical bulky groups (see Chart 1).

2. Computational methods

Geometries were fully optimized with hybrid density functional theory at the B3LYP [13,14] and B3PW91 [13,15] levels using the GAUSSIAN 98 and 03 programs [16]. Many basis sets were tested for B3LYP and B3PW91 calculations. As the reasonable basis sets, 6-311+G(2df) for Si and Ga, 6-311G(d) for Na, and 6-31G(d) for C and H were employed: all these basis sets are incorporated in the GAUSSIAN package [16].

3. Results and discussion

3.1. Substituent effects on RSi≡SiR

We have first carried out the geometry optimization of RSi≡SiR for R = Si*i*PrDis$_2$, since its structure has been determined by X-ray crystal analysis [9]. The crystal structure shows that Dis$_2$*i*PrSiSi≡SiSi*i*PrDis$_2$ has C_2 symmetry.

Table 1
Bond distances (Å) and angles (°) of the C_2 structure of RSi≡SiR (R = Si*i*PrDis$_2$) at several levels of theory

	Si–Si	∠Si–Si–R	∠R–Si–Si–R
B3LYP			
3-21G*	2.072	137.3	172.4
6-31G(d)	2.093	136.8	173.7
6-311G(d)[Si]:6-31G(d)[C,H]	2.091	136.4	177.7
6-311G(2d)[Si]:6-31G(d)[C,H]	2.090	136.6	178.3
6-311+G(2d)[Si]:6-31G(d)[C,H]	2.088	137.2	173.9
6-311G(2df)[Si]:6-31G(d)[C,H]	2.084	137.9	175.4
6-311+G(2df)[Si]:6-31G(d)[C,H]	2.082	136.4	175.7
6-311G(3d)[Si]:6-31G(d)[C,H]	2.085	137.3	175.4
6-311+G(3d)[Si]:6-31G(d)[C,H]	2.085	137.2	173.6
6-311G(3df)[Si]:6-31G(d)[C,H]	2.083	137.8	179.3
6-311+G(3df)[Si]:6-31G(d)[C,H]	2.081	138.0	173.3
B3PW91			
3-21G*	2.070	137.2	179.6
6-31G(d)	2.086	138.0	169.7
6-311G(d)[Si]:6-31G(d)[C,H]	2.082	138.2	170.0
6-311G(2d)[Si]:6-31G(d)[C,H]	2.081	138.6	171.2
6-311+G(2d)[Si]:6-31G(d)[C,H]	2.081	138.5	169.8
6-311G(2df)[Si]:6-31G(d)[C,H]	2.077	139.2	171.0
6-311+G(2df)[Si]:6-31G(d)[C,H]	2.077	139.0	169.7
6-311G(3d)[Si]:6-31G(d)[C,H]	2.078	138.5	170.7
6-311+G(3d)[Si]:6-31G(d)[C,H]	2.078	138.4	169.7
6-311G(3df)[Si]:6-31G(d)[C,H]	2.076	139.0	179.2
6-311+G(3df)[Si]:6-31G(d)[C,H]	2.075	139.2	169.6
Expl.[a]	2.062	137.4	179.5

[a] Taken from Ref. [9].

However, the structure with C_i symmetry was also optimized as an energy minimum. Key geometrical parameters optimized for the C_2 and C_i structures are summarized in Tables 1 and 2, respectively, together with the experimental values. At any level of calculations, the C_2 and C_i structures differ little in the central Si–Si bond distance and Si–Si–R bond angle, except the difference of ca. 10° in the R–Si–Si–R dihedral angle. In addition, it was calculated that the energy differences between the C_2 and C_i structures are only 0.1–0.5 kcal/mol. Therefore, we focus on the C_2 structure that is observed in the crystal structure.

As Table 1 shows, the central Si–Si bond distance optimized with the small 3-21G* basis set agrees rather well with the experimental value, though this agreement is probably due to basis set superposition errors. The larger 6-31G(d) basis set makes the Si–Si distance significantly longer than the experimental value, though it is generally employed as a standard basis set. As the basis set on Si becomes larger, the Si–Si distance becomes shorter and closer to the experimental value. In contrast, the basis-set dependence is very small for the Si–Si–R and R–Si–Si–R angles. As is apparent from Table 1, B3PW91 gives a better result than B3LYP. It can be calculated at the B3PW91/6-311+G(2df)[Si]: 6-31G(d)[C,H] level that the Si–Si distance is only 0.015 Å (0.013 Å with 6-311+G(3df) on Si) longer than the experimental value. The slightly shorter Si–Si distance in the crystal structure is probably ascribed to packing forces because of the bulk of the Si*i*PrDis$_2$ group, as

Table 2
Bond distances (Å) and angles (°) of the C_i structure of RSi≡SiR (R = Si*i*PrDis$_2$) at several levels of theory

	Si–Si	∠Si–Si–R	∠R–Si–Si–R	ΔE[a]
B3LYP				
3-21G*	2.072	136.0	180.0	−0.37
6-31G(d)	2.092	136.2	180.0	−0.12
6-311G(d)[Si]:6-31G(d)[C,H]	2.088	136.0	180.0	−0.06
6-311G(2d)[Si]:6-31G(d)[C,H]	2.087	136.4	180.0	−0.10
6-311+G(2d)[Si]:6-31G(d)[C,H]	2.088	136.3	180.0	−0.23
6-311G(2df)[Si]:6-31G(d)[C,H]	2.084	137.0	180.0	+0.09
6-311+G(2df)[Si]:6-31G(d)[C,H]	2.083	137.0	180.0	−0.23
6-311G(3d)[Si]:6-31G(d)[C,H]	2.084	136.4	180.0	+0.02
6-311+G(3d)[Si]:6-31G(d)[C,H]	2.084	136.0	180.0	−0.24
6-311G(3df)[Si]:6-31G(d)[C,H]	2.081	137.0	180.0	+0.08
6-311+G(3df)[Si]:6-31G(d)[C,H]	2.081	137.2	180.0	−0.18
B3PW91				
3-21G*	2.068	137.6	180.0	−0.10
6-31G(d)	2.085	137.3	180.0	−0.41
6-311G(d)[Si]:6-31G(d)[C,H]	2.081	137.2	180.0	−0.46
6-311G(2d)[Si]:6-31G(d)[C,H]	2.080	137.6	180.0	−0.44
6-311+G(2d)[Si]:6-31G(d)[C,H]	2.082	137.9	180.0	−0.40
6-311G(2df)[Si]:6-31G(d)[C,H]	2.076	138.2	180.0	−0.45
6-311+G(2df)[Si]:6-31G(d)[C,H]	2.077	138.2	180.0	−0.50
6-311G(3d)[Si]:6-31G(d)[C,H]	2.077	137.6	180.0	−0.46
6-311+G(3d)[Si]:6-31G(d)[C,H]	2.078	137.4	180.0	−0.52
6-311G(3df)[Si]:6-31G(d)[C,H]	2.074	138.7	180.0	−0.37
6-311+G(3df)[Si]:6-31G(d)[C,H]	2.074	138.4	180.0	−0.47

[a] $\Delta E = E(C_i \text{ structure}) - E(C_2 \text{ structure})$ in kcal/mol.

will be discussed latter for the Ga–Ga distance in $Na_2[Ar^*GaGaAr^*]$.

The structures of RSi≡SiR optimized for R = Tbt, Ar* and SiMe(Si*t*Bu$_3$)$_2$ as well as R = Si*i*PrDis$_2$ at the B3PW91/6-311+G(2df)[Si]:6-31G(d)[C,H] level are shown in Fig. 1. Key geometrical parameters, natural charge densities, binding energies, and isomerization energies are summarized in Table 3. The central Si–Si distances of 2.077 and 2.080 Å calculated for R = Si*i*PrDis$_2$ and SiMe(Si*t*Bu$_3$)$_2$ are 0.05–0.06 Å shorter than those of 2.128 and 2.138 Å for R = Tbt and Ar*. This reflects that the Si*i*PrDis$_2$ and SiMe(Si*t*Bu$_3$)$_2$ groups are electropositive while Tbt and Ar* are electronegative, as indicated by the natural charge densities (Q_{Si}) on the central Si atoms. The Si–Si distance in RSi≡SiR is also correlated with the doublet-quartet energy difference (ΔE_{DQ}) of the SiR component [2a,2b,2c,2f]. As is shown in Table 3, the ΔE_{DQ} values of 18.9 and 25.6 kcal/mol calculated for R = Si*i*PrDis$_2$ and SiMe(Si*t*Bu$_3$)$_2$ are much smaller than those of 43.7 and 48.1 kcal/mol for R = Tbt and Ar*. The smaller ΔE_{DQ} values for R = Si*i*PrDis$_2$ and SiMe(Si*t*Bu$_3$)$_2$ are due to the electropositive character that helps to decrease the size difference between the valence s and p orbitals on the Si atom of SiR [2a,2b,2c,2f].

For comparison, the geometrical parameters of RSi≡SiR optimized for R = H, Me, and SiH$_3$ are also given in Table 3. It is interesting that the Si–Si distances

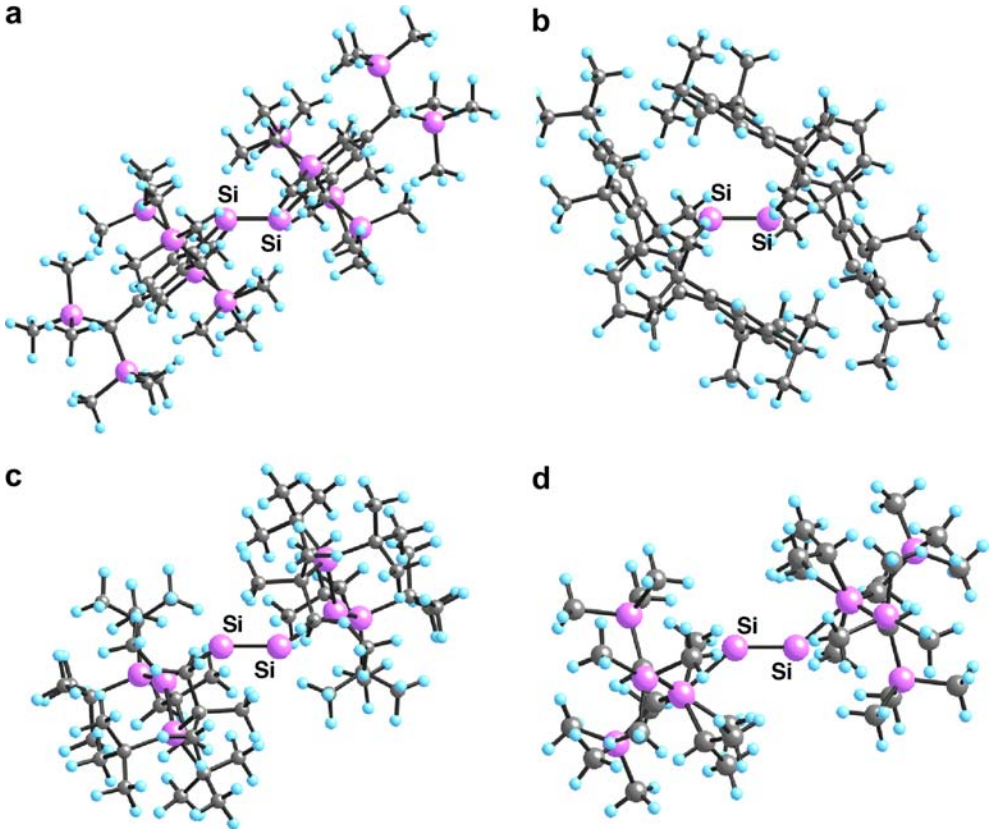

Fig. 1. The optimized structures of RSi≡SiR (R = Tbt (a), Ar* (b), SiMe(Si*t*Bu$_3$)$_2$ (c), and Si*i*PrDis$_2$ (d)) at the B3PW91/6-311+G(2df)[Si]:6-31G(d)[C,H] level.

Table 3
Geometrical parameters, binding energies (BE), natural charge densities (Q_{Si}), and isomerization energies (IE) of RSi≡SiR at the B3PW91/6-311+G(2df)[Si]:6-31G(d)[C,H] level

R	H	CH_3	SiH_3	Bulky aryl groups		Bulky silyl groups	
				Tbt	Ar*	$SiMe(SitBu_3)_2$	$SiiPrDis_2$
Symmetry	C_{2h}	C_2	C_{2h}	C_i	C_2	C_2	C_2
Si–Si (Å)	2.093	2.103	2.082	2.128	2.138	2.080	2.077
∠Si–Si–R (°)	125.5	130.0	130.6	134.8	131.6	148.8	139.0
∠R–Si–Si–R (°)	180.0	178.7	180.0	180.0	171.8	180.0	169.7
Q_{Si}[a]	0.120	0.360	−0.044	0.355	0.432	−0.074	−0.126
BE (kcal/mol)[b]	62.1	58.2	71.3	43.0	32.1	49.7	66.6
ΔE_{DQ} (kcal/mol)[c]	37.3	41.2	21.2	43.7	48.1	25.6	18.9
IE (kcal/mol)[d]	−7.5	−7.0	−4.9	30.2	44.7	33.7	34.9

[a] The natural density on the central Si atom.
[b] $BE = 2E(SiR) - E(RSi{\equiv}SiR)$.
[c] $\Delta E_{DQ} = E(\text{quartet SiR}) - E(\text{doublet SiR})$.
[d] $IE = E(SiSiR_2) - E(RSi{\equiv}SiR)$.

of 2.077 and 2.080 Å for R = Si*i*PrDis$_2$ and SiMe(Si*t*Bu$_3$)$_2$ are rather shorter than those of 2.093, 2.103, and 2.082 Å for R = H, CH_3, and SiH_3, respectively, despite the bulk of the Si*i*PrDis$_2$ and SiMe(Si*t*Bu$_3$)$_2$ groups. This is because Si*i*PrDis$_2$ and SiMe(Si*t*Bu$_3$)$_2$ groups are more electropositive than SiH_3, while H and Me are electronegative. Si*i*PrDis$_2$ and SiMe(Si*t*Bu$_3$)$_2$ groups have a higher SOMO level than SiH_3, and the *i*PrDis$_2$ and Me(Si*t*Bu$_3$)$_2$ parts in Si*i*PrDis$_2$ and SiMe(Si*t*Bu$_3$)$_2$ are more negatively charged than the H_3 part in SiH_3. It should be noted that the ΔE_{DQ} value for the most electropositive Si*i*PrDis$_2$ is smaller than those of 21.2, 37.3 and 41.2 kcal/mol for SiH_3, H, and Me.

It may be argued that RSi≡SiR has a tendency to dissociate in solution, as R becomes bulkier. Therefore, the binding energies (BE) required to cleave the central Si–Si bond (leading to two SiR fragments in the ground doublet state) were calculated, as shown in Table 3. The BE values are 66.6 and 49.7, and 43.0 kcal/mol for R = Si*i*PrDis$_2$, and SiMe(Si*t*Bu$_3$)$_2$, and Tbt, respectively, confirming that the central two Si atoms are strongly bonded. It is interesting that BE is also correlated with ΔE_{DQ}, as shown in Table 3. The BE value for R = Ar* is somewhat smaller but still as large as 32.1 kcal/mol.

Obviously, bulky groups help to destabilize the 1,2-R shifted isomer $SiSiR_2$, because two bulky R groups crowd more around one end of the Si–Si bond. Thus, RSi≡SiR was calculated to be more stable than $SiSiR_2$ by 30.2, 33.7, 34.9, and 44.7 kcal/mol for R = Tbt, SiMe(Si*t*Bu$_3$)$_2$, Si*i*PrDis$_2$, and Ar*, respectively. These energy differences are large enough to prevent isomerization as well as dimerization (the dimerization leading to a cyclobutadiene analogue was calculated to be 25, 42, 50, and 82 kcal/mol endothermic for R = Si*i*PrDis$_2$, Tbt, SiMe(Si*t*Bu$_3$)$_2$, and Ar* at the B3LYP/3-21G* level, respectively.).

As well known, RC≡CR has a linear structure owing to sp hybridization, and the C–C triple bond consists of one σ bond and two π bonds. However, silicon has a low tendency to form ideal sp hybrid orbitals because of the size difference between valence s and p orbitals [2a,2b,2c,2f]. As a result, RSi≡SiR prefers to take a trans-bent structure. In the trans-bent structure, the central Si–Si bond consists of a somewhat distorted σ bond, an out-of-plane π_{out} bond, and a slipped in-plane π_{in} bond. The slipping of π_{in} is due to the fact that the low-lying vacant σ* orbital is mixed into π_{in} upon trans-bending, as known as a second-order Jahn-Teller effect. The mixing of σ* into π_{in} contributes to the stabilization of the trans-bent structure, but makes the π bond weakened because of the antibonding character of σ*. As a result, the total Si–Si bond order becomes less than three. Therefore, there has been much debate on the bonding contribution of the slipped π_{in} bond (for very recent arguments of the nature of the triple bond in RE≡ER, see Ref. [17]). As Fig. 2 shows, it is interesting that the slipped π_{in} orbitals of RSi≡SiR for R = Si*i*PrDis$_2$ and SiMe(Si*t*Bu$_3$)$_2$ have more significant bonding character between the central Si atoms, as a result of the smaller ΔE_{DQ} values of the SiR components [2a,2b,2c,2f], than those for R = Tbt and Ar*, which help to form a triple bond.

The energy levels of σ, π_{out}, and π_{in} orbitals as well as the counterparts σ*, π_{out}*, and π_{in}* are shown in Fig. 3. Substituent effects on the reactivities of RSi≡SiR toward reagents will be discussed elsewhere in due course.

3.2. Substituent effects on $Na_2[RGaGaR]$

The X-ray crystal study of $Na_2[Ar^*GaGaAr^*]$ by Robinson and co-workers showed that the Ga–Ga distance is as short as 2.319 Å [10]. A close value of 2.324 Å was also reported by Power and co-workers from the X-ray crystal study [18]. A number of theoretical calculations were performed to discuss the nature of the Ga–Ga distance by replacing the bulky Ar* group by small groups such as H, CH_3, and Ph [11]. All the Ga–Ga distances calculated for the simplified model systems are 0.1–0.2 Å longer than the experimental values, when calculations were done at high levels with large basis sets. Cotton and co-workers carried out calculations for the more realistic model system by replacing the *i*Pr groups on Ar* by H atoms (i.e., using C_6H_3-2,6-Ph_2), and suggested that attractive interactions between Na cations and terphenyl groups shorten the Ga–

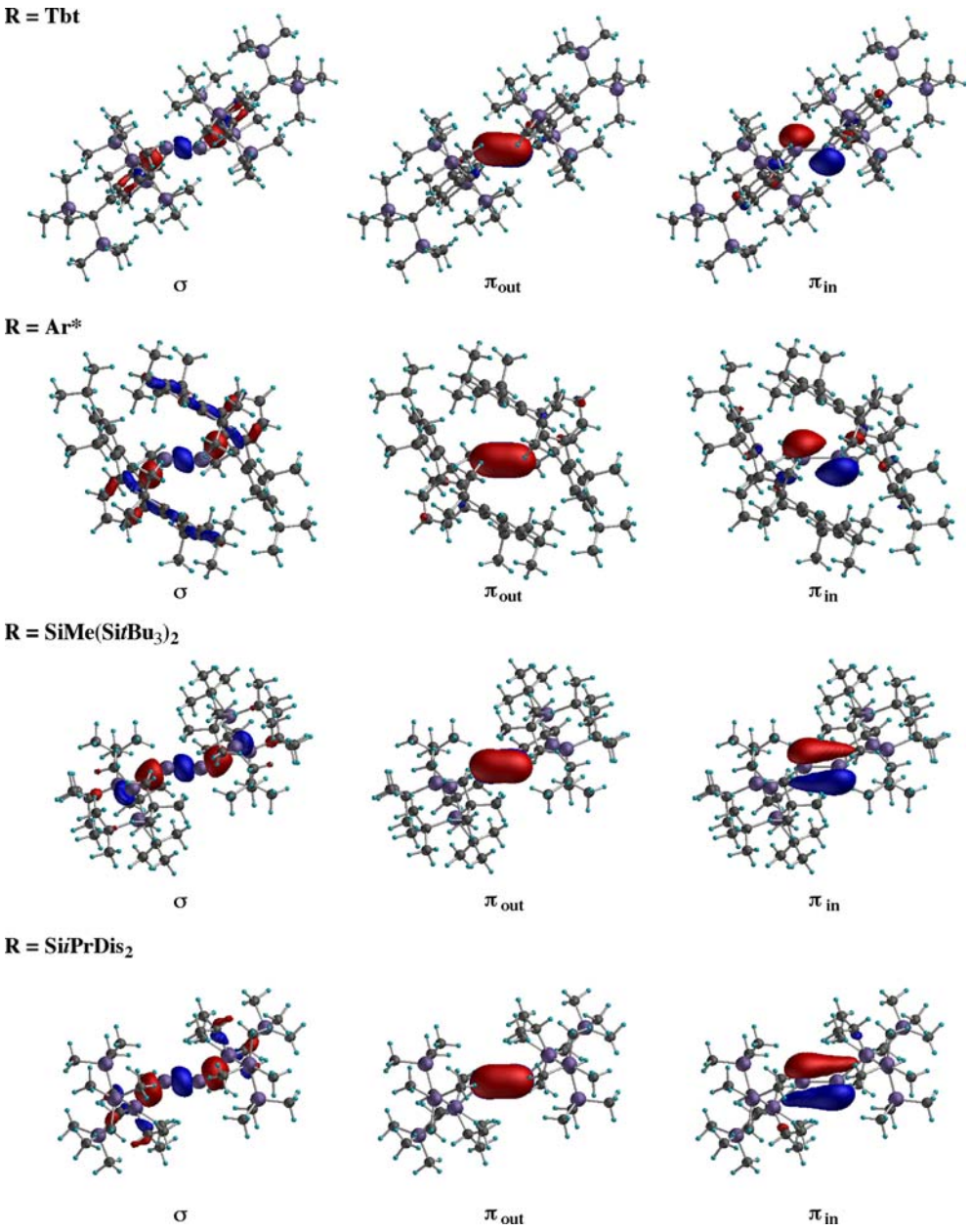

Fig. 2. The σ, π_{out}, and π_{in} orbitals of RSi≡SiR at the B3PW91/6-311+G(2df)[Si]:6-31G(d)[C,H] level, plotted with a value of 0.05 a.u.

Ga distance [19]. By performing calculations with large basis sets, Xie et al. showed that the Ga–Ga distance is shortened to 2.404 Å [20]. A very similar Ga–Ga distance of 2.402 Å was also calculated in our previous study [12]. However, these Ga–Ga distances are still 0.08–0.09 Å longer than the experimental values of 2.319 [10] and 2.324 [18] Å. It has been suggested that inclusion of the *i*Pr groups is important in shortening the Ga–Ga distance [12].

Thus, we have carried out geometry optimization for the real compound, $Na_2[Ar^*GaGaAr^*]$, at the B3PW91/6-311+G(2df)[Ga]:6-311G(d)[Na]:6-31G(d)[C,H] level, as shown in Fig. 4. Key geometrical parameters are given in Table 4, together with the experimental values by Robinson [10] and Power groups [18]. The Ga–Ga distance was calculated to be 2.344 Å, this being closer to the experimental values of 2.319 [10] and 2.324 Å [18], but still 0.02–0.03 Å longer. This discrepancy may be ascribed to an error in calculation methods. However, it is important to note that the optimized structure of $Na_2[Ar^*GaGaAr^*]$ has C_2 symmetry and its two Ga–Ga–Ar* angles are equivalent (133.5°), while the Ga–Ga–Ar* angles are not equivalent (128.5° vs. 133.5° [10] and 125.9° vs. 134.0° [18]) in the crystal structures as a result of molecular deformations due to crystal packing effects.

In the meantime, Power and co-workers synthesized the closely related compound, $Na_2[Ar'GaGaAr']$, and determined its structure by X-ray crystal analysis [21]. The Ar′ and Ar* groups differ in the fact that Ar′ (=C_6H_3-2,6-(C_6H_3-2,6-*i*Pr_2)$_2$) has no *i*Pr group at the para-positions in both terminal sides of the terphenyl group. Therefore,

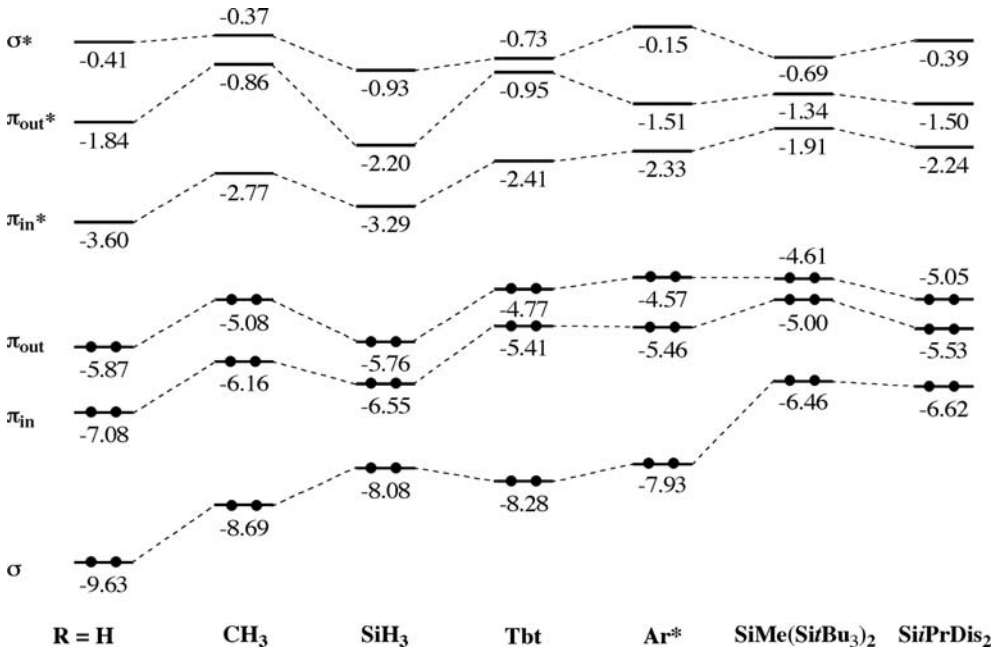

Fig. 3. Orbital levels (eV) of RSi≡SiR at the B3PW91/6-311+G(2df)[Si]:6-31G(d)[C,H] level.

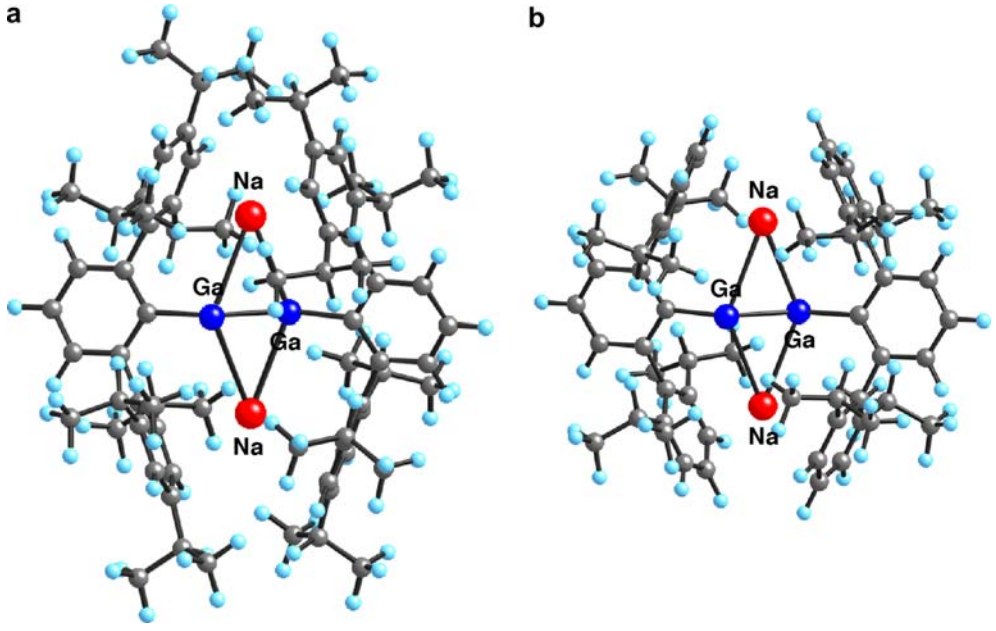

Fig. 4. The optimized structures of Na_2[RGaGaR] (R = Ar* (a) and Ar′ (b)) at the B3PW91/6-311+G(2df)[Ga]:6-311G(d)[Na]:6-31G(d)[C,H] level.

the spatial expanding of Ar′ is smaller than that of Ar*. It is noticeable that Na_2[Ar′GaGaAr′] has C_2 symmetry even in the crystal structure, unlike the Ar* case. Geometry optimization also shows that Na_2[Ar′GaGaAr′] has C_2 symmetry. The optimized Ga–Ga distance of 2.342 Å agrees within 0.005 Å with the experimental value of 2.347 Å in the crystal structure of Na_2[Ar′GaGaAr′]. In addition, the optimized Ga–Ga–R angle of 133.9° agree well with that of 130.7° in the crystal structure. These indicate that the present calculations are sufficiently reliable, and suggest that the crystal structure of Na_2[Ar*GaGaAr*] is much more affected by packing forces. Thus, the difference of 0.023 Å in the experimental Ga–Ga distances of Na_2[Ar′GaGaAr′] and Na_2[Ar*GaGaAr*] agree very well with the discrepancy of 0.020 Å between experiment and calculation for Na_2[Ar*GaGaAr*]. The present calculations suggest that Na_2[Ar′GaGaAr′] and Na_2[Ar*GaGaAr*] have almost the same Ga–Ga distance in the absence of crystal packing forces [22].

In an attempt to assess how Na_2[Ar*GaGaAr*] is structurally pliable, geometry optimization was carried out by fixing the Ga–Ga distance and Ga–Ga–Ar* angles at the

Table 4
Key geometrical parameters and natural charge densities (Q) of Na_2[RGaGaR] (R = Ar* and Ar′) at the B3PW91/6-311+G(2df)[Ga]:6-311G(d)[Na]:6-31G(d)[C,H] level

	Ar*			Ar′	
	Expl.[a]	Expl.[b]	Calc.	Expl.[c]	Calc.
Symmetry	C_1	C_1	C_2	C_2	C_2
Ga–Ga (Å)	2.319	2.324	2.344	2.347	2.342
Ga–Na (Å)	3.078, 3.085	3.065, 3.103	3.094	3.058	3.082
	3.056, 3.106	3.085, 3.102	3.100	3.101	3.091
∠Ga–Ga–R (°)	128.5, 133.5	125.9, 134.0	133.5	130.7	133.9
∠R–Ga–Ga–R (°)			174.9		176.5
Q_{Ge}			−0.328		−0.314
Q_{Na}			0.899, 0.904		0.894, 0.897

[a] Taken from Ref. [10].
[b] Taken from Ref. [18].
[c] Taken from Ref. [22].

experimental values. The resultant structure is only 0.7 kcal/mol less stable than the fully optimized structure. This suggests that the potential energy surface is very flat for the changes in the Ga–Ga distance and Ga–Ga–Ar* angles. Therefore, it is natural that the Ga–Ga distance of Na_2[Ar*-GaGaAr*] is significantly affected by crystal packing forces, because Ar* is bulkier, though the reasons for the different Ga–Ga distances in the crystal structures of Na_2[Ar*GaGaAr*] and Na_2[Ar′GaGaAr′] have remained obscure [21].

4. Conclusion

For disilyne (RSi≡SiR), several effects of bulky aryl (Tbt and Ar*) and silyl (Si*i*PrDis$_2$ and SiMe(Si*t*Bu$_3$)$_2$) groups are disclosed and characterized by density functional calculations with large basis sets. Silyl groups help to make the Si–Si triple bond shorter. However, the aryl-substituted disilyne is also an interesting synthetic target. For the short Ga–Ga distance observed for Na_2[Ar*GaGaAr*], it is revealed that crystal packing forces as well as other factors such as attractive interactions between Na and Ar* play an important role, as suggested by the density functional calculation showing that Na_2[Ar*GaGaAr*] and Na_2[Ar′GaGaAr′] have almost the same Ga–Ga distance. In general, crystal structures (as well as crystallization) are significantly affected even by delicate changes in the bulk of substituent groups.

Acknowledgements

This work was supported by the Grant-in-Aid for Scientific Research on Priority Area (Reaction Control of Dynamic Complexes) and Creative Scientific Research from the Ministry of Education, Culture, Sports, Science, and Technology of Japan.

References

[1] (a) R. Okazaki, R. West, Adv. Organomet. Chem. 39 (1996) 231;
(b) P.P. Power, J. Chem. Soc., Dalton Trans. (1998) 2939;
(c) M. Weidenbruch, Eur. J. Inorg. Chem. (1999) 373;
(d) P.P. Power, Chem. Rev. 99 (1999) 3463;
(e) P. Jutzi, Angew. Chem., Int. Ed. 39 (2000) 3797;
(f) M. Weidenbruch, J. Organomet. Chem. 646 (2002) 39;
(g) P.P. Power, Chem. Commun. (2003) 2091;
(h) M. Weidenbruch, Angew. Chem., Int. Ed. 42 (2003) 2222;
(i) M. Weidenbruch, Angew. Chem., Int. Ed. 44 (2005) 514.
[2] (a) K. Kobayashi, S. Nagase, Organometallics 16 (1997) 2489;
(b) S. Nagase, K. Kobayashi, N. Takagi, J. Organomet. Chem. 611 (2000) 264;
(c) K. Kobayashi, N. Takagi, S. Nagase, Organometallics 20 (2001) 234;
(d) N. Takagi, S. Nagase, Organometallics 20 (2001) 5498;
(e) N. Takagi, S. Nagase, Chem. Lett. (2001) 966;
(f) N. Takagi, S. Nagase, Eur. J. Inorg. Chem. (2002) 2775;
(g) N. Takagi, K. Yamazaki, S. Nagase, Bull. Korean Chem. Soc. 24 (2003) 832 (a special issue).
[3] (a) M. Stender, A.D. Phillips, R.J. Wright, P.P. Power, Angew. Chem., Int. Ed. 41 (2002) 1785;
(b) M. Stender, A.D. Phillips, P.P. Power, Chem. Commun. (2002) 1312.
[4] Y. Sugiyama, T. Sasamori, Y. Hosoi, Y. Furukawa, N. Takagi, S. Nagase, N. Tokitoh, J. Am. Chem. Soc. 128 (2006) 1023.
[5] (a) A.D. Phillips, R.J. Wright, M.M. Olmstead, P.P. Power, J. Am. Chem. Soc. 124 (2002) 5930;
(b) L. Pu, A.D. Phillips, A.F. Richards, M. Stender, R.S. Simons, M.M. Olmstead, P.P. Power, J. Am. Chem. Soc. 125 (2003) 11626.
[6] L. Pu, B. Twamley, P.P. Power, J. Am. Chem. Soc. 122 (2000) 3524.
[7] (a) N. Wiberg, W. Niedermayer, G. Fischer, H. Nöth, M. Suter, Eur. J. Inorg. Chem. (2002) 1066;
(b) N. Wiberg, S.K. Vasisht, G. Fischer, P. Mayer, Z. Anorg. Allg. Chem. 630 (2004) 1823.
[8] M. Karni, Y. Apeloig, N. Takagi, S. Nagase, Organometallics 24 (2005) 6319.
[9] A. Sekiguchi, R. Kinjo, M. Ichinohe, Science 305 (2004) 1755.
[10] J. Su, X.-W. Li, R.C. Crittendon, G.H. Robinson, J. Am. Chem. Soc. 119 (1997) 5471.
[11] (a) K.W. Klinkhammer, Angew. Chem., Int. Ed. Engl. 36 (1997) 2320;
(b) M.M. Olmstead, R.S. Simons, P.P. Power, J. Am. Chem. Soc. 119 (1997) 11705;
(c) R. Dagani, Chem. Eng. News 76 (March 16) (1998) 31;
(d) I. Bytheway, Z. Lin, J. Am. Chem. Soc. 120 (1998) 12133;
(e) Y. Xie, R.S. Grev, J. Gu, H.F. Schaefer III, P.v.R. Schleyer, J. Su, X.-W. Li, G.H. Robinson, J. Am. Chem. Soc. 120 (1998) 3773;
(f) G.H. Robinson, Acc. Chem. Res. 32 (1999) 773;
(g) R.B. King, G.H. Robinson, J. Organomet. Chem. 597 (2000) 54;
(h) J. Grunenberg, N. Goldberg, J. Am. Chem. Soc. 122 (2000) 6045;

(i) H. Grützmacher, T.F. Fässler, Chem. Eur. J. 6 (2000) 2317;
(j) R. Köppe, H. Schnöckel, Z. Anorg. Allg. Chem. 626 (2000) 1095;
(k) G.H. Robinson, Chem. Commun. (2000) 2175;
(l) T.L. Allen, W.H. Fink, P.P. Power, J. Chem. Soc., Dalton Trans. (2000) 407;
(m) J. Grunenberg, J. Chem. Phys. 115 (2001) 6360;
(n) H.-J. Himmel, H. SchnÖckel, Chem. Eur. J. 8 (2002) 2397;
(o) P.P. Power, Struct. Bonding 103 (2002) 57;
(p) D.B. Chesnut, Heteroatom Chem. 14 (2003) 175;
(q) R. Ponec, G. Yuzhakov, X. Gironés, G. Frenking, Organometallics 23 (2004) 1790.

[12] N. Takagi, M.W. Schmidt, S. Nagase, Organometallics 20 (2001) 1646.

[13] (a) A.D. Becke, Phys. Rev. A 38 (1988) 3098;
(b) A.D. Becke, J. Chem. Phys. 98 (1993) 5648.

[14] C. Lee, W. Yang, R.G. Parr, Phys. Rev. B 37 (1988) 785.

[15] J.P. Perdew, Y. Wang, Phys. Rev. B 45 (1992) 13244.

[16] M.J. Frisch, G.W. Trucks, H.B. Schlegel, G.E. Scuseria, M.A. Robb, J.R. Cheeseman, J.A. Montgomery, Jr., T. Vreven, K.N. Kudin, J.C. Burant, J.M. Millam, S.S. Iyengar, J. Tomasi, V. Barone, B. Mennucci, M. Cossi, G. Scalmani, N. Rega, G. A. Petersson, H. Nakatsuji, M. Hada, M. Ehara, K. Toyota, R. Fukuda, J. Hasegawa, M. Ishida, T. Nakajima, Y. Honda, O. Kitao, H. Nakai, M. Klene, X. Li, J.E. Knox, H.P. Hratchian, J.B. Cross, C. Adamo, J. Jaramillo, R. Gomperts, R.E. Stratmann, O. Yazyev, A.J. Austin, R. Cammi, C. Pomelli, J.W. Ochterski, P.Y. Ayala, K. Morokuma, G.A. Voth, P. Salvador, J.J. Dannenberg, V.G. Zakrzewski, S. Dapprich, A.D. Daniels, M.C. Strain, O. Farkas, D.K. Malick, A.D. Rabuck, K. Raghavachari, J.B. Foresman, J.V. Ortiz, Q. Cui, A.G. Baboul, S. Clifford, J. Cioslowski, B.B. Stefanov, G. Liu, A. Liashenko, P. Piskorz, I. Komaromi, R.L. Martin, D.J. Fox, T. Keith, M.A. Al-Laham, C.Y. Peng, A. Nanayakkara, M. Challacombe, P.M.W. Gill, B. Johnson, W. Chen, M.W. Wong, C. Gonzalez, J.A. Pople, Gaussian, Inc., Wallingford CT, 2004.

[17] (a) M. Lein, A. Krapp, G. Frenking, J. Am. Chem. Soc. 127 (2005) 6290;
(b) C.A. Pignedoli, A. Curioni, W. Andreoni, ChemPhysChem 6 (2005) 1795;
(c) G. Frenking, A. Krapp, S. Nagase, N. Takagi, A. Sekiguchi, ChemPhysChem 7 (2006) 799;
(d) C.A. Pignedoli, A. Curioni, W. Andreoni, ChemPhysChem 7 (2006) 801.

[18] (a) B. Twamley, P.P. Power, Angew. Chem., Int. Ed. 39 (2000) 3500;
(b) N.J. Hardman, R.J. Wright, A.D. Phillips, P.P. Power, J. Am. Chem. Soc. 125 (2003) 2667.

[19] F.A. Cotton, A.H. Cowley, X. Feng, J. Am. Chem. Soc. 120 (1998) 1795.

[20] Y. Xie, H.F. Schaefer III, G.H. Robinson, Chem. Phys. Lett. 317 (2000) 174.

[21] N.J. Hardman, R.J. Wright, A.D. Phillips, P.P. Power, Angew. Chem., Int. Ed. 41 (2002) 2842.

[22] The same trend is also expected for the key geometrical parameters of Ar′Si≡SiAr′ (Si–Si = 2.140 Å, ∠Si–Si–R = 131.8°, and ∠R-Si–Si–R = 177.8°) and Ar*Si≡SiAr* (Table 3) in the absence of crystal packing forces.